MAIN RESULTS OF AIRBORNE SOUNDING OF AEROSOL CONDUCTED AT THE INSTITUTE OF ATMOSPHERIC OPTICS FROM 1981 TILL 1991

B.D. Belan, V.E. Zuev, and M.V. Panchenko

Institute of Atmospheric Optics,
Siberian Branch of the Russian Academy of Sciences, Tomsk
Received July 14, 1994

A review of main results of atmospheric aerosol study obtained at IAO since 1981 with airborne laboratory is presented. The data of aerosol spatiotemporal variability, microphysics, and composition, as well as a description of some atmospheric phenomena where the aerosol plays a leading role are given in the paper. Aerosol of anthropogenic origin is also considered.

The benefits of using airborne instrumentation for measurements in the atmosphere came to the attention of physicists since the advent of aviation. Apparently, the use of meteorograph onboard the aircraft in Frankfurt am Main in 1912 may be considered as the start of airborne sounding of the atmosphere.[1] In Russia regular airborne sounding was started in 1921, and then in the USA, France, Norway, Sweden, and other countries.[2]

The airborne sounding is now one of the basic techniques for investigating the atmosphere primarily because the present aircraft are capable of delivering many sensors and instruments combined into a unified information and measuring system at large altitudes, conducting the measurements supported with software, energy, and metrology, and accommodating as many experimentators as required. The airborne sounding data are very reliable since the aircraft can directly penetrate the spatial volume under study. The advantages of this technique are in the integrated character of airborne experiments, i.e., the possibility of measuring air physical characteristics simultaneously that makes looking for relations between them easier. The aircraft—laboratory allows tracking the examined atmospheric phenomenon for a distance of thousands kilometres and thus keeping watch on evolution of its characteristics. Tens of special and multi—purpose airborne laboratories have been created all over the world. Characteristics of the majority of them are given in Ref. 3.

What has been said above served as a basis for the airborne technique to be put into practice of the scientific—research work at the Institute of Atmospheric Optics. In the middle 1970s the airborne sounding was occasionally used at the Institute and mainly intended to construct aircraft facilities for measuring the atmospheric parameters and develop the techniques for sounding characteristics of air and underlying surface. This sounding became regular since 1981. From 1985 till 1988 it was near the monitoring regime. In this paper we generalize the results obtained during airborne sounding of atmospheric aerosols within the span of ten years from 1981 till 1991.

INSTRUMENTATION AND REGIONS UNDER STUDY

Over the period of 1981—1991 the soundings were accomplished with an IL—14 aircraft laboratory (see Ref. 4) mainly in the background regions and were devoted to studying the atmospheric aerosol. The aircraft—laboratory incorporated such measuring complexes as the meteorological and microphysical ones,[5] a nephelometer PhAN with thermo— and hydro—optical instruments,[6] a nephelometer of external volume,[7] spectrophotometric complex,[8] an airborne recording system,[9] and lidars of several modifications.[10]

After the termination of the IL—14 aircraft service the scientific instrumentation complex was mounted onboard an AN—30 carrier in 1988 without substantial change. Only the units intended for outside operation were modified since the AN—30 aircraft differs from the IL—14 aircraft by its tightness. The AN—30 aircraft possesses some advantages as compared to IL—14. These are higher altitudes, large load—carrying capacity and power/displacement ratio, as well as the presence of five optical hatches intended for input and output of optical radiation.[3] The aircraft—laboratory AN—30 was used in the same applications as IL—14, and it operated till the end of 1989.

Severe ecological situation in many regions of the USSR brought about the need in reorientation of aircraft program at the Institute of Atmospheric Optics. The reconstructed AN—30 aircraft—laboratory was named "OPTIK—E" (ecological). The detailed description of "OPTIK—E" as well as of its further modification "OPTIK—EM" is given in Ref. 11. During the period between 1989 and 1991 the aircraft—laboratory was used for survey of the air quality over different cities and territories, including the works done by orders of municipal bodies.

Since detailed information about these studies and can be found in Refs. 4—11 here we give, in Table I, only basic specifications of the measuring complexes. In addition arrangement of the whole instrumentation set up installed on board an AN—30 aircraft is shown in Fig. 1. It should be noted that Table I lists the data only on constantly measured parameters. The instruments used onboard the aircraft occasionally are not included in the Table I.

TABLE I. Specifications of scientific instrumentation mounted onboard the aircraft—laboratories of the Institute of Atmospheric Optics.

| System or instrument	Parameter	Range	Error	Note
Navigation system	flight course air speed ground speed drift angle bank angle pitch angle g—load altitude	0—360° 0—600 km/hr 0—800 km/hr − 30−+ 30° − 45−+ 45° − 22−+ 22° − 1.5 g—+ 1.5 g 0—8100 m	2° 10 km/hr 10 km/hr 2° 2° 1° 0.02 g 20 m	
Meteorological system	temperature humidity pressure wind speed wind direction	− 70−+ 50°C 10—100% 800—200 Torr 0—300 km/hr 0—360°	0.5°C 7% 1 mm Hg 20 km/hr 5°	
Thermodynamic system	fluctuations of temperature and wind over 3 coordinates	0—100 Hz		still under development
Photoelectric counter AZ—5	disperse composition	0—300 cm^{-3} 0.4—10 μm	20%	12 channels
Diffusion battery DCA	disperse composition	0—1 000 cm^{-3} 3—200 μm	20%	8 channels
Nephelometer FAN with thermo— and hydro—optics	aerosol extinction	0.001—1 km^{-1} 10—400°C 10—100%	7% 1°C 5%	
Filter ventilated system	chemical composition of aerosol	10—250 l/min	5%	Analysis in the laboratory
Ozonometer OZ—P GIAM—15 GIAM—15 IRF—2	O_3 CO_2 CO_2 gamma—background	1—1000 μg/m^3 1—100 ppm 10—1000 ppm 1—1000 μR/hr	10% 5% 10% 20%	
Lidar	depth of water sounding water extinction coefficient aerosol concentration	2—30 m 0.1—0.5 m^{-1} 10—1700 μg/m^3	2.2 m 20% 20%	
Spectrophotometer	upwelling radiation	0.44—1.62 μm	20%	8 channels
Radiometer	radiative temperature	8.1—14.8 μm 250—320 K	 1 K	5 channels
Thermovision system	radiative temperature	− 20—1600°C	1°C	
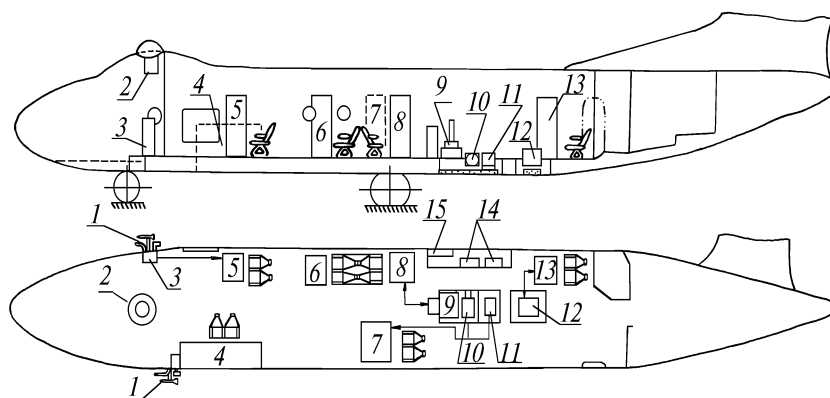
FIG. 1. Arrangement of instrumentation onboard an "OPTIK − E" AN—30 aircraft—laboratory: 1) units of air samplers and sensors, 2) solar spectrometer, 3) rack of preliminary transformers of gas and aerosol complex, 4) chromatograph, 5) nephelometer with thermo— and hydro—optical means, 6) central computer, 7) recording system of the spectrophotometrer, 8) recording system of the lidar, 9) lidar, 10) spectrophotometer, 11) radiometer, 12) thermovision system, 13) recording system of the thermovision system, 14) electric dashboard, and 15) navigation complex.

FIG. 2. Regions of operation of the aircraft—laboratories of the Institute of Atmospheric Optics: •— points of obtaining vertical profiles, ⊙ — cities where complex ecological sounding was made, ≡— the same for territories, and ⊡ − expeditions and special experiments.

TABLE II. Regions of operation of aircraft—laboratory and flight time.

Year	Aircraft	West Siberia	East Siberia	European part of the USSR	Kazakhstan	Ural	Far East	Middle Asia	Number of air samples	Number of hours
1981	IL—14	+	+	−	+	−	−	−	108	130
1983	<<	+	+	−	+	−	−	−	136	190
1984	<<	+	+	+	+	+	−	+	121	420
1985	<<	+	+	+	+	−	−	−	508	860
1986	<<	+	+	+	+	−	+	+	470	1160
1987	<<	+	+	+	+	+	−	+	670	1020
1988	<<	+	+	+	+	+	−	+	249	320
	AN—30	+	+	+	+	−	+	+	349	520
1989	<<	+	+	+	+	+	+	+	563	420
1990	<<	+	+	+	+	+	+	+	244	320
1991	<<	+	+	−	−	+	+	+	356	145
1981— 91	IL—14 AN—30	+	+	+	+	+	+	+	3774	5505

In the period from 1981 to 1991 the soundings were carried out almost in all geographic and administrative regions of the former USSR using the aforementioned aircraft—laboratories. This is seen from the map presented in Fig. 2. The statistics of flights over different parts of this map is naturally different. Thus, e.g., for the territory of West Siberia, where Tomsk, i.e., a place of aircraft—laboratory base, is situated, the repetition rate of measurements is the highest. In some regions there are only single profiles. Table II gives the most exact information about the regions where the sounding was accomplished as well as about flight time and the number of air samples taken for their analysis.

Moreover, the aircraft—laboratories of the Institute of Atmospheric Optics were used in the integrated experiments: "Vertical'—86" and "Vertical'—87" (West Siberia), OdAeks—87 (Odessa), Soviet—American dust experiment "Dyuna—89" (Dushanbe). Using these aircraft—laboratories we examined the state of the air basin over Kamchatka, Lake Baykal and the Baykal region, Buriatiya, oil deposits of Megion and Samotlor, as well as over Nizhny Tagil, Nizhnevartovsk, Pavlodar, Ust'—Kamenogorsk, Amursk, Khabarovsk, Komsomols'k—on—Amur, Ulan Ude, and Kemerovo.

SPATIOTEMPORAL VARIABILITY OF AEROSOL

The instrumentation complexes of the aircraft—laboratories of the Institute of Atmospheric Optics allowed us to solve problems of different scales in space and time, i.e., from fluctuation (microscale) variations to long—term variations occurring in the atmosphere. Let us demonstrate this. First let us consider the map of suspended matter distribution over the former USSR averaged over the period between 1981 and 1991 (Fig. 3). Data of vertical sounding of the atmosphere in different geographical regions were used to make the map. The data were time—averaged. The vertical extension of the layer measured changed from 0.1 to 8 km. However, the data were averaged over 0—3 km layer in which the overwhelming bulk of aerosol was concentrated. The profiles obtained in the regions exposed to the effect of industrial centers were excluded from the data processing.
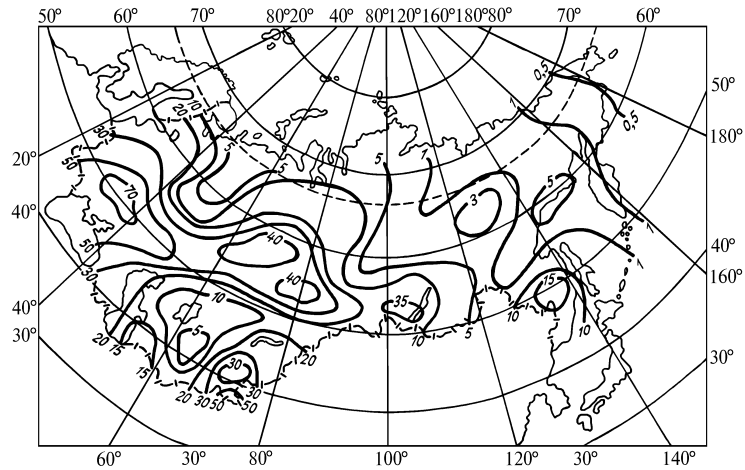
FIG. 3. Distribution of the aerosol particle number density ($\overline{N} = \frac{1}{H}\int\limits_{0}^{H} N(h)\mathrm{d}h$) over the territory of the former USSR.

It can be seen from Fig. 3 that several zones of enhanced content of suspended matter can be isolated in the mixing layer over the territory under study. The principal zone is located over the west regions of the European part of the USSR and it is caused by addition of the enhanced background concentrations of aerosol being transferred from West Europe and from emissions of the Donetsk–Dnepropetrovsk industrial zone taking into account the west–to–east transfer of the aerosol.

The effect of this zone spreads to the southern regions of East Siberia. It should be noted that the strengthening effect of the Ural industrial zone is added as well as the effect of the industrial plants located in the Northern Kazakhstan and southern West Siberia. This effect manifests itself as appearance of two additional zones of enhanced aerosol concentration. The background concentration of suspended particles in the region effected by Irkutsk industrial zone is somewhat lower. One more quite clearly pronounced zone of enhanced aerosol concentration ($N > 50$ cm^{-3}) is over the territory of the Middle Asian republics. Its appearance can be explained by air stagnation in the mountain valleys where the industrial enterprises are concentrated.

In spite of the fact that we have excluded all the profiles measured over the "caps" of the industrial cities from data processing, Fig. 1 shows that now the anthropogenic activity determines the regional background of pollution.

The regional background can also be inhomogeneous that is seen from aerosol distribution over the territory of West Siberia depicted in Fig. 4. The conditions of mapping were identical to those in Fig. 3. It is seen that in addition to two zones indicated above (Ural zone and the south zone of West Siberia), one more zone appears in the Nizhnevartovsk–Strezhevoi region because of the emissions due to combustion of the accompanying gases in the plumes over oil deposits. In addition, there is a narrow zone of a relatively low aerosol concentration ($N = 50$ cm^{-3}) in the center of West Siberia. This zone lies between two pollution sources located to the north and to the south of the region. In our opinion, the mean distribution shown in Fig. 4 underlines the need for regional monitoring of each territory.

The regional spatial inhomogeneity of aerosol number density distribution depicted in Figs. 3 and 4 is also manifested in its other characteristics, i.e., chemical composition, particle size distribution, etc.
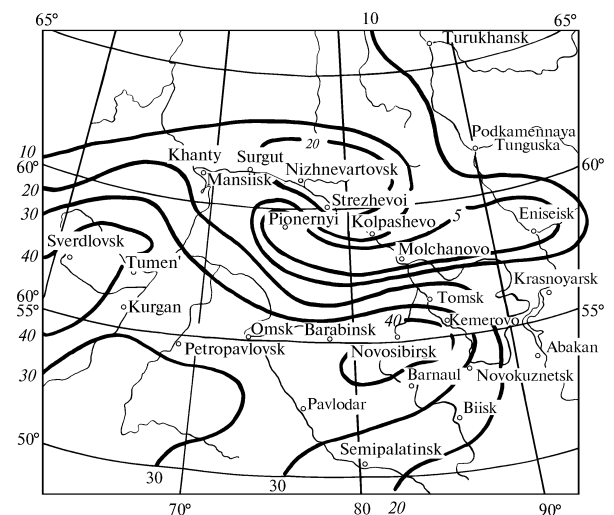

FIG. 4. Distribution of the aerosol number density over West Siberia.

Figure 5 represents mean concentrations of different chemical components of aerosol substance for three regions such as Kamchatka, West Siberia, and Kazakhstan. West Siberia and Kazakhstan were chosen because of the greatest number of samples (867 and 642, respectively) collected. As for Kamchatka, it is marked by the lowest particle number density (Fig. 3) which can be classified as a natural aerosol. The number of samples for this region is 167.

The analysis of data from Kamchatka revealed that aerosol particles over this region possess two basic sources of formation, i.e., sea surface (Na$^+$, K$^+$, Cl$^-$, and NH$_4^+$) and underlying surface of the peninsula (Fe, Mg, Al, Ca, and Si).
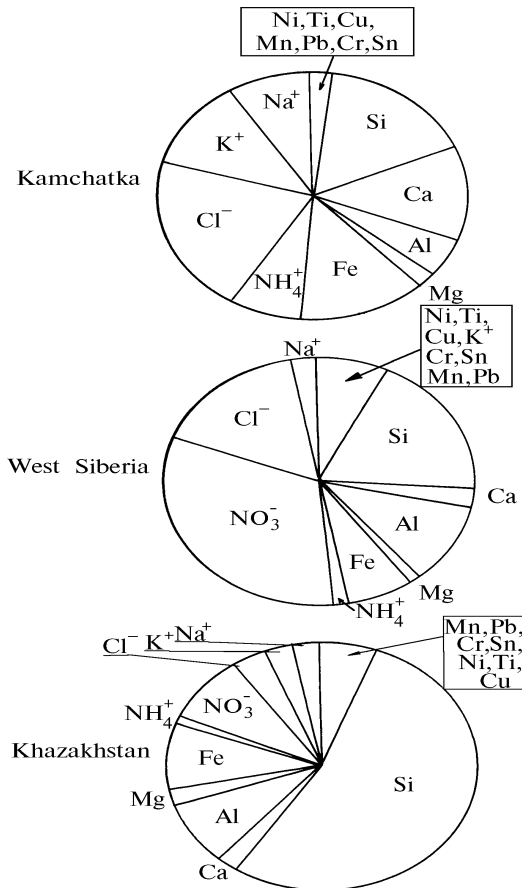
FIG. 5. Chemical composition (%) of aerosol over different regions (Kamchatka, West Siberia, and Kazakhstan).

As indicated earlier (Figs. 3 and 4), West Siberia, especially its South, is affected by anthropogenic discharges from local sources, and it possesses high background of admixtures brought by the system of west—to—east transport. This is clearly manifested in sharp increase of concentration of such components as Cl^- and NO_3^-. The concentration of soil fraction also increases with the increase of total concentration.

Kazakhstan is in an intermediate position here. All of the three fractions can be separated out in aerosol over this region. They are the marine, soil, and photochemical (anthropogenic) ones that can be accounted for by the proximity of the Caspian and Aral Seas and the existence of large industrial objects in its territory. Sharp increase of Si concentration over this region can be explained by the presence of vast deserts with a sandy surface.

For many practical applications it is important to know not only true aerosol distribution but its microscale inhomogeneities and a character of its concentration fluctuations. The aerosol field statistical characteristics were studied with the use of airborne complex of the IL—14 aircraft—laboratory (air speed was 70 m/s). The complex components described in Refs. 4, 5, 7, and 9 were used. The information record rate for nephelometer was 10 Hz, for AZ—5 and mean meteoparameter sensors it was 1 Hz, and for temperature fluctuation sensor it was 100 Hz. The data were processed using the algorithms which are usually used for analyzing turbulent characteristics of the atmosphere.[12]

During the flights at different altitudes over different regions of the former USSR we revealed some general regularities in the behavior of correlation functions of the backscattering coefficient and of the number density N of aerosols which bear information on the spatial structure of aerosol fields. The shapes of correlation functions R_β and R_N essentially depend on flight altitude and diameter d of aerosol particles. At the same time, no strong dependence of the correlation function R_β on wavelength is observed in the range between 0.37 and 0.7 μm.

Depicted in Fig. 6 are the correlation functions of the backscattering coefficient and aerosol number density derived during one of the flights in June 1984 over West Siberia. The spatial radii of correlation estimated at the level 0.5 are 7—15 m for the backscattering coefficient and 30—150 m for number density. Clearly seen in the figure is the altitude—dependence of correlation radii. Thus, the higher the level at which the correlation function has been calculated the smaller are the scales of aerosol inhomogeneities. For the backscattering coefficients at an altitude of 400 m $L(R_\beta = 0.5) = 15$ m and at 3200 m $L(0.5) = 7$ m. The same regularity is evident from the data on the aerosol particle number density, i.e., $H = 500$ m and $L(R_N = 0.5) = 120$ m, $H = 4600$ m, $L(0.5) = 40$ m.
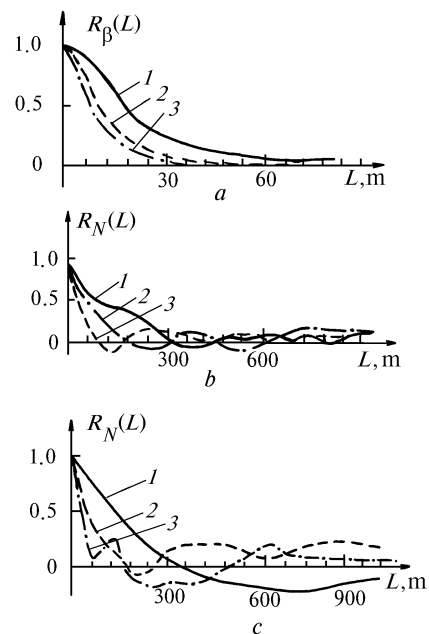

FIG. 6. Spatial normalized autocorrelation functions of: a) backscattering coefficient (λ = 0.7 μm) at altitudes of 400 (1), 1500 (2), and 3200 m (3); b) number density (d≥0.4 μm) at altitudes of 500 (1), 2600 (2), and 4600 m (3); and, c) at altitude of 1500 m for particles of d≥0.4 (1), 0.7 (2), and 1 μm (3).

Similar dependences were observed for Kazakhstan, Ural, and East Siberia. The characteristic scales of aerosol inhomogeneities also slightly depend on aerosol particle number density which sometimes could differ in its values by more than one order of magnitude. The decrease of specific aerosol inhomogeneity size with altitude is of an objective character that is supported by results obtained using essentially different methods.

One of the physical reasons for the formation of altitude dependence of correlation functions is incomplete entrainment

of aerosol particles with turbulent flows.[13] In this case, one should take into account the fact that the time of particle relaxation with respect to the flow which entrains it depends not only on its size but also on the ratio of a particle size to air molecule free path. Under the experimental conditions (see Fig. 6) the air molecule free path increases with height by a factor of 1.4 at the most. However, this does not fully explain the altitude variation of aerosol correlation radii presented in the figure.

The decrease of characteristic scale of inhomogeneities with the altitude increase can also be caused by the decrease of the coefficient of air turbulent diffusion. Both of these factors can act simultaneously. Values of aerosol particle number density for different–size particles and backscattering coefficients at different wavelengths between 0.37 and 0.7 μm at fixed altitudes were recorded to determine the priority of the considered mechanisms of influence on aerosol. The results on concentration fluctuations obtained during a flight over Kazakhstan in December, 1984 (Fig. 6c) reveal the decrease of aerosol inhomogeneity size with the particle size increase. This allows us to judge on the priority of the first hypothesis since the coefficient of air diffusion can be considered constant at a given altitude. For particles of $d>0.4$ μm the inhomogeneity scale at the level $R_N(L) = 0.5$ was 140 m. This regularity occurs at all altitudes and is also of universal character. It was supported by the data obtained over the European territory of the former USSR, West Siberia, and Ural and can be observed in data on number density of different–size aerosol particles presented in Ref. 14 in which the authors did not make the corresponding statistical generalizations.

As known,[15] if we consider the fluctuation spectra of the majority of meteorological parameters in a wide frequency interval exceeding the inertial one, then a mesoscale minimum can be found in them. The transition from an inertial to mesoscale interval is determined by outer scale of turbulence. The spectral interval used in this paper is insufficient to cover such a large interval. However, the spectral density curves show bends which characterize the transition from the ”−5/3” law on the obtained fluctuation spectra of the backscattering coefficient and aerosol particle number density.
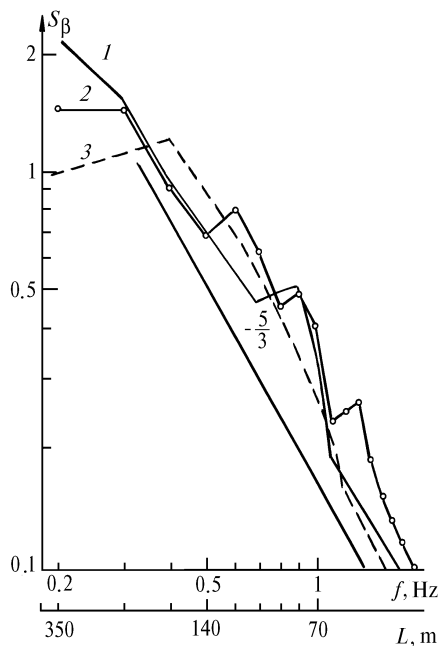

FIG. 7. Spectral density of backscattering coefficient fluctuations ($\lambda = 0.7$ μm) at altitudes of 500 (1), 3000 (2), and 4600 m (3).
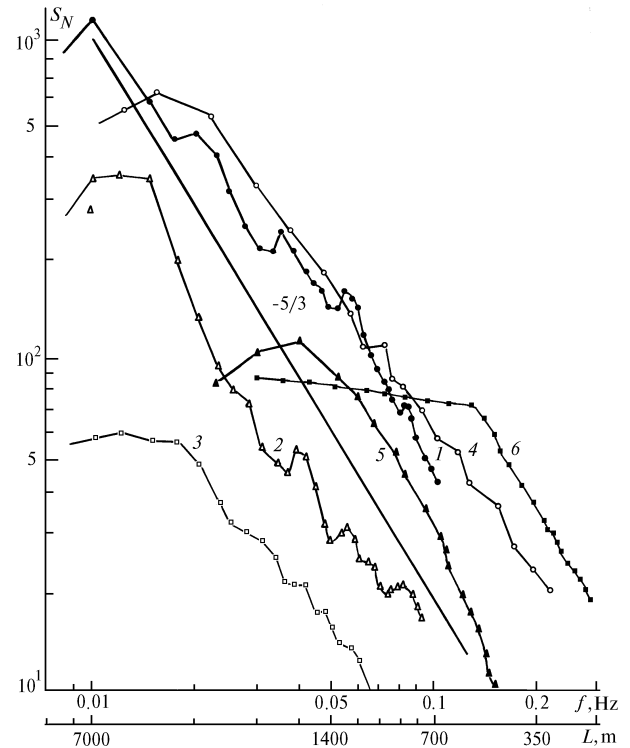

FIG. 8. Spectral density of the aerosol number density fluctuations ($d{\geq}0.4$ μm) at altitudes of 500 (1), 2000 (2), and 4500 m (3) and at altitude of 2500 m for particles of $d{\geq}0.4$ (4), 1.0 (5), and 4.0 μm (6).

Figures 7 and 8 show that the fluctuation spectra of the backscattering coefficient and aerosol concentration follow the ”−5/3” law and starting from some frequency interval show a bend. It should be noted that this bend is altitude–dependent. If we transfer to spatial periods, it turns out (Fig. 7) that $S_{\beta}(L)$ at an altitude of 500 m follows the ”−5/3” law on the interval to 350 m. As the height increases this interval narrows and at an altitude of 4600 m the lower boundary of the interval becomes equal to 0.4 Hz or to the 175 m scale. The same regularity is observed in the curves of spectral density of aerosol number density fluctuations (Fig. 8, curves 1−3).

Substantial difference in the outer scales of the backscattering coefficient number density can be accounted for by a decisive contribution of large aerosol particles, whose concentration is small, to scattered optical signal fluctuations. Figure 8 (curves 4−6) shows variation of spatial scale interval, in which the spectral density of aerosol number density fluctuations follows the ”−5/3” law, depending on the aerosol particle size. As seen from the figure, the larger the size of aerosol particles, the higher is the lower frequency of the interval of the ”−5/3” law. Thus, if the outer scale for particles with $d>1$ μm is 1600 m (curve 5), for particles $d>4$ μm L_0 is 350 m (curve 6). The differences between the spectra obtained for other physico–geographical regions are reduced to variations in the outer scale L_0 limiting the ”−5/3” law interval. It is possible to assume that the bend in the curves of spectral density characterizes the largest size of eddies which influence efficiently the aerosol field at a given altitude or the specific size of particles.

Thus, the experimental study of correlation functions of aerosol inhomogeneities and spectra of aerosol

concentration fluctuations confirms the validity of the basic principles of the theory and simultaneously separates out those factors which cannot be explained. These factors are altitude variations of aerosol inhomogeneities and spectra of aerosol concentration fluctuations.

One of the most important climatic characteristics of the atmospheric parameters is their temporal variability which is determined by diurnal and annual behavior and interannual tendencies. For atmospheric aerosol, the diurnal behavior specifies a rate of generation, accumulation, and sink of particles caused by change from day to night. The annual behavior determines the same characteristics depending on insolation variations. The long–term trends caused by the aforementioned parameters and macroscale circulation, which plays a role of feedback, manifest themselves in the interannual tendencies.

Examination of diurnal and annual behavior of aerosol vertical distribution revealed that during a day the profiles change most strongly in the lower 500–m layer of air (the inner mixing layer[7]) where they follow, as a rule, the temperature profile.[18] The annual behavior is specified by the maximum concentration in spring and the deep minimum between September and December which is determined by the behavior of photochemical processes.[18]

The most interesting result concerning the dynamics of aerosol is a long–term behavior of its vertical distribution depicted in Fig. 9. As is seen from this figure the aerosol concentration over West Siberia decreased to 1988 and then increased, this increase was particularly sharp in 1991.

In the climate theory some variations in the meteorological parameters with periods exceeding one year are known.[15] The curve shown in Fig. 9 most likely follows the 11–year cycle. As known, the character of atmospheric circulation can also change in this case. The analysis of aerosol chemical composition for the period under study showed that the aerosol concentration decreased at the cost of its mineral fraction, especially, such components as Al, Ca, and Fe. A portion of ions Na^+ and K^+ during the same period increased. It suggests that a smaller portion of continental air masses and a larger potion of marine masses arrived at the territory of West Siberia, i.e., air circulation changed.
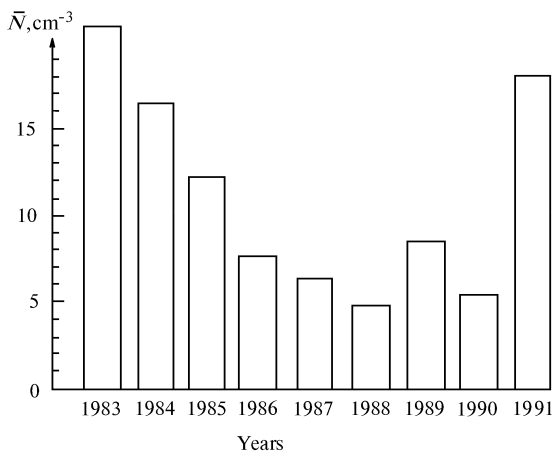

FIG. 9. Long–term behavior of aerosol particle number density over West Siberia ($\overline{N} = \frac{1}{H}\int_0^H N(h)\mathrm{d}h$).

It should be noted in conclusion that the data base was developed as a result of the long–term sounding of

aerosol.[19] It became a basis for constructing regional microphysical models of aerosols which were used for grounding of optical models of the atmosphere by Krekov and Rakhimov.[20]

STUDY OF SOME PROCESSES AND PHENOMENA

The regular airborne sounding accomplished in the 1980's enabled us not only to store extensive data sets but also to investigate individual atmospheric processes and phenomena which were not described in the literature. We will not describe all of the results in detail. Only the most important of them are presented in this paper.

The stored data on aerosol vertical distribution made it possible to study the climatic dynamics of the mixing layer and its inner layer[17] and the processes of particle accumulation in them.[23] In particular, the internal mixing layer is shown to retain the aerosol supply into the main mixing layer as long as the particles fully occupy the inner one.

The examination of "fine" stratification of aerosol under the temperature inversion conditions has revealed the formation of layers some meters thick with elevated aerosol concentration which coincide with the levels of sharp change of temperature gradients (both in the positive and negative direction) and in which there occurs strong turbulence.[22]

As to aerosol layers, they can move in the vertical direction as a unifield layer and keep their parameters.[23] The direction and velocity of their movement inside a homogeneous air mass can be determined with high precision using the adiabatic method of calculating vertical movements.[24]

During the sounding of microphysical parameters of dust layer in the experiment "Dyuna" we obtained for the first time their vertical distribution and showed that inside this layer ozone sink took place on particles of suspended matter.[25–27]

The examination of aerosol moisture content under different physico–geographical conditions in the free atmosphere revealed its nonuniqueness over different regions and its dependence on chemical composition of particles.[28]

The experimental verification of Mazin hypotheses[29] on the effect of clouds on an aerosol field around them showed that the clouds really shifted the particle–size spectrum towards larger particles.[30]

The comparison of the data on aerosol microphysics with those of direct measurements of its optical characteristics demonstrated good agreement which can be expressed as[31]

$$\sigma_{aer}(0.55) = 3.4 \cdot 10^{-2} N + 0.011 \ ,$$

where $\sigma_{aer}(0.55)$ is the volume scattering coefficient (km^{-1}) at $\lambda = 0.55$ μm, and N is the number density of particles of $r \geq 0.2$ μm (cm^{-3}).

During the airborne sounding of the atmosphere two atmospheric phenomena which have not been described before were observed.

One of them is the presence of closed air circulation in the Baykal hollow along its contour. At the same time the basic flow from the west is observed over Lake Baykal. This phenomena is described at length in Ref. 32.

The second phenomenon is the formation of aerosol clouds at low relative humidity. It was observed for the first time in 1981 (see Refs. 33–37). Here we describe only its generalized characteristics.

As known, when there are no clouds the aerosol above the boundary layer is distributed sufficiently uniformly in the atmosphere. From the data on the backscattering coefficient[16,18] and aerosol particle number density it is possible to separate out inhomogeneities not exceeding some hundreds of meters or large–scale ingomogeneities of some thousand kilometres in the aerosol horizontal distribution.[38] In the range from some kilometres to some hundred kilometres the so–called mesoscale minimum of aerosol scattering fluctuations and, consequently, aerosol number density is observed.

The aerosol clouds detected during the airborne sounding differ strongly from conventional water or crystal ones and, in their absence, from aerosol distribution in free atmosphere. The main feature of this phenomenon is that in a clear dry atmosphere (relative air humidity lower than 40%) at altitudes higher than 1000 m, i.e., in the layer above the inversion, the localized areas with elevated aerosol number density are observed with a horizontal scale from units to tens of kilometres.

TABLE III. Characteristics of noncondensational aerosol clouds.

Region, period	Time	Horizontal size, km	Altitude, km	Air temperature, °C	Relative humidity, %	$\dfrac{N_{cl}}{N_{air}}$	Note
West Siberia:							
07.XII.1983	17.08–	16	2.25	− 20.06	35	5	Field of 11 clouds
14.XII.1983	17.12	9–6	1.84	− 16.4−−17.0	16 − 22	4 − 9	
16.XII.1983	15.40–	15	1.70	− 9.1	24	40	
20.XII.1983	17.10	12	1.45	− 12.7	16	20	
12. V.1984	14.30–	20	1.2–1.8	+ 4.0−− 3.0	24 − 28	7.5	
15. V.1984	14.34	7–8	2.25	− 10.7−− 11.2	26 − 33	4− 5	Field of 2 clouds
20.IX.1985	16.55–	12	1.10	+ 20.1 + 22.5	28 − 31	8	
18.XII.1986	16.58	20	2.60	− 24.0 − 25.6	22 − 35	3	
14. V.1987	22.56–	21	2.80	+ 2.0−+ 2.4	19 − 22	4	
	2345						
	19.48–						
	20.04						
	15.15–						
	15.32						
	22.58–						
	23.21						
	17.17–						
	17.43						
Kazakhstan:							
27.VI.1984	22.34–	24	2.53	+ 7.0−+ 7.5	30 − 36	5	
29.VI.1984	22.40	18	4.53	− 4.1−− 4.9	20 − 24	6	
29.VI.1984	04.18–	8 − 14	3.40	+ 1.6−+ 2.3	28 − 30	7 − 9	Field of 6 clouds
10.IV.1985	04.34	35	2.70	− 9.2−− 9.7	22 − 24	4	
04.VI.1986	20.57–	8 − 16	2.30	− 1.0−− 4.2	27 − 33	3 − 4	Field of 6 clouds
	22.00						
	07.10–						
	07.48						
	01.25–						
	03.58						
Ural:							
12.XII.1984	19.00–	20	1.80	− 7.0−− 7.2	32 − 33	10	
12.XII.1984	19.05	20	1.80	− 6.7−− 7.2	27 − 31	6	
	21.05–						
	21.10						
Middle Asia:							Field of 8 clouds
11.XII.1981	16.52–	2 − 16	2.75	0.0−− 1.2	24 − 25	5 − 8	Hygrometer did not
05.II.1986	17.50	24(48)	2.70	− 5.5−− 6.2	50	65	record humidity lower
	22.57–						than 50 %
	23.30						
West Siberia:							
13.V.1984	19.00–	10 − 12	2.40	− 12.7−− 13.0	36 − 39	5 − 8	Field of 3 clouds
	19.58						
Baykal region:							
20.IX.1986	13.14–	8	2.70	+ 0.2−+ 1.0	46 − 49	5	
	13.30						
Far East:							
26.IX.1986	13.58–	10	3.00	−0.4−0.8	24 − 27	3	
	14.12						
Total:		6–35(48)	1.1…4.5 3	− 25.6…+ 27.5	16…39(49)	3…65	

Note: N_{cl}/N_{air} is the ratio of the aerosol number density in the cloud to that in the ambient air.

First we present the table in which the cases of occurrence of aerosol noncondensational clouds recorded to date are listed (Table III). As follows from Table III, during the flights the conditions of the formation of 21 noncondensational aerosol clouds were recorded. Three more clouds were detected as a reality. Based on the data tabulated we describe a general pattern of the formation of these clouds.

The temporal distribution of occurrences of the aerosol noncondensational clouds is not uniform. As a rule, over most of territories they were observed in the afternoon and late in the evening. The exception is the region of Kazakhstan where one case was recorded at night and two cases in the morning.

As also follows from Table III, such formations could be observed over any area where the flights were carried out. This is indicative of sufficiently general physical nature of this phenomenon.

Horizontal dimensions of such clouds vary between 6 and 35 km, in one case it was 48 km but a core of 24 km can be separated out in it. The mean value of horizontal extension is 8 to 20 km that is conmensurate with the clouds of vertical development.[39,40]

The altitude at which such formations were observed can also be different. It varies between 1.1 and 4.53 km. They were not recorded below 1.1 km that can be accounted for by the fact that the clouds are not distinguished against the general background inside the mixing layer where aerosol concentration is high.

The temperature range at which the noncondensational clouds were detected was extremely wide, i.e., between −25.6 and +22.5°C that shows once more the universal origin of the phenomenon detected.

The particle number density increases by a factor of 3 to 65 in a cloud as compared to that in the ambient air. As to its mean value it is between 5 and 8. The same relations are specific for usual water droplet clouds as well.[41]

Noncondensational clouds can be observed both as individual clouds and as fields. Of 24 cases six cases fall on the fields of such clouds. The largest number of clouds in that set was 11.

The clouds detected differ from the usual water droplet or crystal ones in that they are observed under low relative humidity which is, as a rule, $f < 40\%$.

It is seen from Table III that in one case the humidity was 46–49% and in the other case the hydrometer did not record the humidity lower than 50% for some technical reasons. As known,[39,41] at such relative humidity, the clouds, in their classical sense, cannot be formed or exist for a long time.

It is important to notice that all cases of noncondensational aerosol clouds were observed far from cities or industrial centers above the inversion layer that excludes their anthropogenic origin.

The vertical extension, based on the data obtained to date can vary between 300 m and 3 km. However, there are few statistical data on this parameter since such atmospheric situations occur very seldom (one case for 160 flight hours). So the well defined criteria which can be used for carrying out the specific flights are not available. As to the conventional flights, they are not intended for flying in the backward direction, therefore, it is impossible to perform multiple flyouths through the area under study.

By way of example, a vertical profile of the aerosol noncondensational cloud depicted in Fig. 10 is taken. It was obtained during the airborne sounding on 14 May, 1987 between 14 hr 20 min and 19 hr 30 min local time over Kolpashevo and Kargasok of Tomsk region. Figure 10a represents distribution of temperature, humidity, and aerosol ($r>0.2$ μm) number density; Fig. 10b shows number density distribution for medium–sized aerosol fraction ($r = 0.50$–0.75 μm).

As is seen from Fig. 10a, the noncondensational cloud is above the inversion layer, and no destructions of the temperature and humidity fields is observed within it. The aerosol concentration inside the cloud is distributed asymmetrically. There is a region with its elevated values in the lower part of the cloud. The asymmetry is more pronounced for individual fractions (Fig. 10b). Thus, while a submicron fraction ($r = 0.20$–0.25 μm) copies roughly the total density distribution ($r \geq 0.20$ μm), the medium–sized fraction ($r = 0.50$–0.75 μm) is localized in a smaller volume, and the core with the largest density adjoins the inversion layer.

The vertical sections of noncondensational aerosol clouds presented in Fig. 10 show that in their shape they are similar to conventional clouds of water drops with vertical development of the Cu or Cb type. The principal difference consists in that the noncondensational clouds are observed in the regions with low relative humidity ($< 50\%$). The lack of condensation is likely to be the mechanism which does not produce deformation of temperature and humidity field inside them.
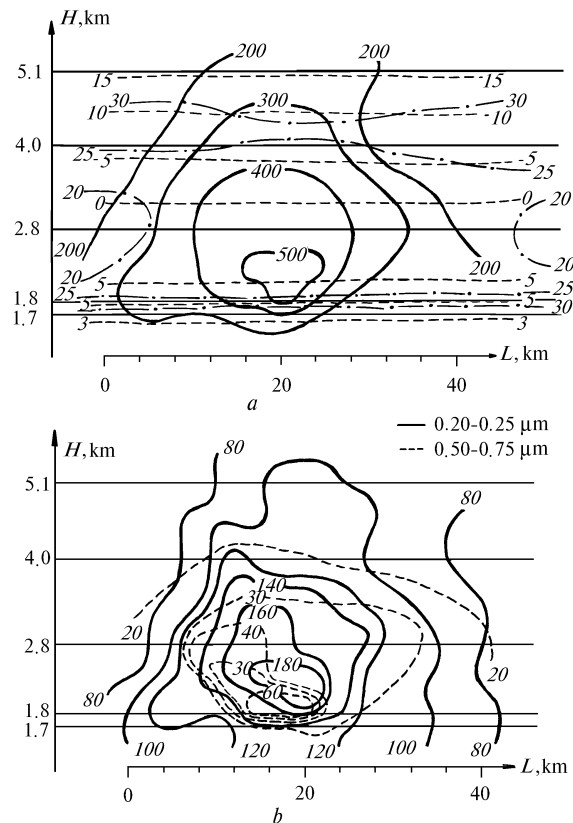

FIG. 10. Noncondensational aerosol cloud: a) distribution of temperature (− − −), humidity (− · −), and aerosol particles number density (bold solid line); aircraft flight levels (solid line); b) particle density distribution: $r = 0.20$–0.25 μm (———————) and $r = 0.50$–0.75 μm (− − − −).

If we consider the aerosol particle size distribution in such clouds and their chemical composition, it is possible to find further differences which are related not only to usual

clouds but also to aerosol existing in the air surrounding the cloud.

The measurements of aerosol particle size distribution inside the cloud and outside it revealed that in the noncondensational cloud there occured not a simple increase of concentration of all aerosol fractions but variation in their ratio. In this case it is possible to separate out the contribution of the medium–sized fraction. Such a situation was observed in all of the ten noncondensational clouds in which the measurements were carried out using a parallel analyzer of particle size distribution. The differences were only in the ratio $N(r = 0.20–0.25\ \mu m)/N(r = 0.5–1\ \mu m)$. In some cases this ratio was 0.4–0.5, otherwise it attained 1.5–1.6. This fact indicates that the medium–sized aerosol particles are of primary importance in the genesis of noncondensational clouds. This is confirmed also by data on the aerosol scattering coefficients ($\lambda = 0.55\ \mu m$) recorded with an air–flow nephelometer and described in Refs. 36 and 37. The increase of the aerosol scattering coefficient with the increase of the total particle number density is accompanied by strong signal fluctuations which are determined by large particles in a small local volume of the nephelometer (~0.5 cm^3).

Different aerosol fractions are known to strongly differ in their chemical composition.[16] The medium and coarse fractions consist mainly of a substance specific for soil particles. The results of determining the aerosol chemical composition inside and outside the cloud are listed in Table IV. It is seen that in a noncondensational cloud the concentration of elements specific for soil particles (Al, Ca, Si, Fe, Ni, Mg, Mn, and Ti) strongly increases while that of photochemical aerosol which is characterized by ions SO_4^{2-}, NH_4^+, NO_3^-, and Cl^-, is below the threshold of detection. It should be noted that the lower threshold of detection of these ions is sufficiently high although in most of samples taken earlier these ions were well identified.

Proceeding from what has been said above it is possible to consider two possible mechanisms of formation of such clouds. The first of them consists in the penetration of overheated local volumes of air through the inversion layer. The second one is the transfer of local volumes of air rich of aerosol through the inversion layer. It is conditioned by mesoscale eddies appearing near the inversion layer due to shearing instability. The results of lidar sounding of aerosol confirm the first mechanism[42] and the results obtained during the dust storm near Dushanbe[25,26] count in favor of the second mechanism.

TABLE IV. *Chemical composition of aerosol* ($\mu g/m^3$) *on February 5–6, 1986 at an altitude of* 2700 m *over Middle Asia.*

Time (local)	Volume, m^3	Al	Ca	Si	Fe	Ni	Mg	Mn	Ti	Na$^+$	K$^+$	Cl$^-$	SO_4^{2-} NH_4^+ NO_3^-	Note
21–26	3.0	0.828	3.915	0.097	0.139	0.166	0.344	0.106	0.028	*	*	*	*	Outside a cloud
23–20	0.3	23.888	22.387	1.116	2.144	1.569	3.156	0.581	0.263	*	*	*	*	Inside a cloud
00–40	7.5	1.012	0.028	0.004	0.025	*	0.033	0.025	0.011	*	0.009	0.927	*	Outside a cloud

ECOLOGICAL STUDIES

Since 1989 the "OPTIK–E" AN–30 aircraft–laboratory performed ecological surveys. It should be noted that such airborne surveys are in common practice.[43–46] However, there were no reliable methodological support. The exception is the problem of studying the transboundary transport, the solution of which is well justified.[47]

The sounding of local areas as well as cities and industrial objects was made, as a rule, based on intuition. Therefore, when proceeding to examination of distribution and dynamics of urban pollutions an effort was undertaken to fill this gap. The methods were developed for determining the balance of substances entering a city from the outside, discharged on its territory, and leaving a city, for mapping the distribution of pollution over the city and in its territory (the latter was measured by a ground–based mobile complex), and for measuring the composition and calculating the amount of emission of large sources.[48]

To determine the pollution balance in a region of a city we needed to measure the mean concentration of pollutants along the perimeter at different altitudes and wind velocity. The balance was estimated by the law of mass conservation in the following form

$$B = \int_l \int_0^H C_i(l,h)V(l,h)\cos(\hat{V},l)\mathrm{d}l\mathrm{d}h$$

or

$$B = \oiint C_i(s)\,V(s)\cos(\hat{V},s)\,\mathrm{d}\,s + \oiint \int_0^H Q_i\,\mathrm{d}s\mathrm{d}h\,,$$

where l is the coordinate along the perimeter of a city, h is the current altitude above the ground, s is the surface element, C_i is the concentration of the pollutant under investigation, V is the wind speed, $\cos(\hat{V},l)$ is the cosine of the angle between the wind direction and the boundary of the region, $\cos(\hat{V},l)$ is the cosine of the angle between the wind direction and the surface element, and Q_i is the rate of generation of the ith pollutant in the territory of a city. The second formula is preferable since it can be used to estimate not only the horizontal balance, but also the vertical one (sedimentation and generation).

This kind of ecological survey of a city follows the scheme shown in Fig. 11a. At first, vertical sounding of the atmosphere is carried out up to the maximum altitude, as shown in the left part of Fig. 11a. It is aimed at determining the temperature and wind stratifications, the height of the mixing layer, and the peculiarities of the vertical profiles of pollutants. Then the aircraft–laboratory flies horizontally along the square or rectangle enclosing a city. The flights are conducted at different altitudes at 100 m intervals from the minimum altitude allowable for the given locality to that of the upper boundary of the mixing layer. The concentration of pollutants at the ground is determined with the help of a ground–based mobile station. In addition to the concentration of pollutants, the meteorological and navigation parameters are recorded during the flight. Independently of the area of the city, this kind of observation should be accomplished in the course of one day at stable weather and wind direction constant in time and altitude. The balance is calculated by any formula given above. The total error in determining the balance

could change from 35 to 60% depending on the selected parameter, weather conditions, and geographical peculiarities of the place. The pollution balances for some cities of the Commonwealth of Independent States (CIS) are given in Ref. 48.

The following kind of operation in urban ecological survey is mapping of the distribution of air and near—ground pollutants. Air pollutants are mapped with the help of the aircraft—laboratory whereas near—ground pollutants — with the help of the mobile station. It is schematically shown in Fig. 11b.

At first, in analogy with the case of balance estimation, vertical sounding is carried out to determine the thermodynamic stratification and the altitude profiles of pollutants. The altitudes of horizontal sections (levels) are selected based on the obtained vertical profiles. These criteria are well known,[49] therefore, we will not dwell on this question. It should be only noted that the mapping altitudes are not *a priori* known except the minimum altitude, but are determined during flights. In this kind of sounding the flight line and the number of flight routes of the aircraft—laboratory are equally spaced. The number of routes can vary from 6 to 12 depending on the area of a city. The number of altitudes can vary from three (under conditions of low ground inversion) to six (under condition of an intense mixing in summer).

The sounding data are subsequently used for mapping of the distribution of different components at every altitude of sounding. Intercomparison of these maps is used to pattern the volume distribution of pollutants over the city, while their temporal variations are used to estimate the dynamics of generation and transfer of pollutants.
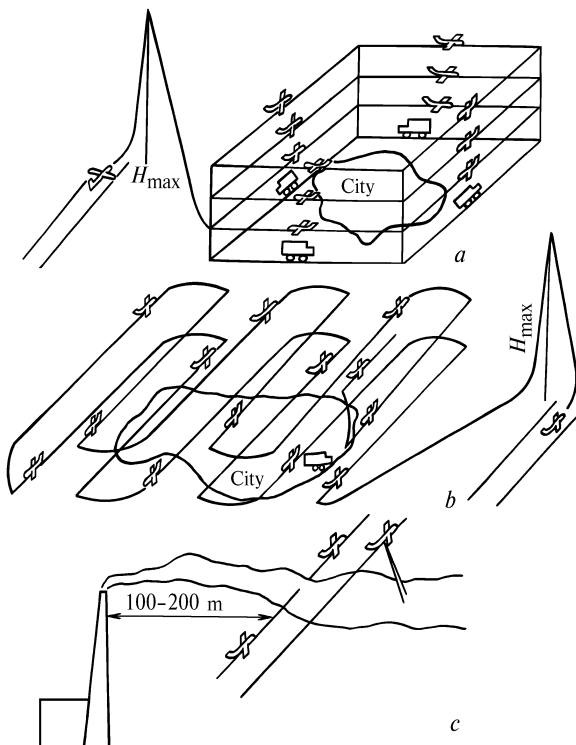

FIG. 11. Schemes of ecological sounding.

In our earlier papers[42,50,51] we gave some examples of maps that demonstrate the peculiarities of the distribution of pollutants over different cities. In addition to this merit, which is more interesting for the specialists on protection of the environment, these maps have one more merit. They can

be used to explain one or the other peculiarity of the obtained distribution by comparing different air characteristics. The above—discussed points are illustrated by Fig. 12 that shows the results of comparison of the aerosol number density distribution over Khabarovsk with the air flow lines at the same altitude.

It can be seen from Fig. 12 that circulations occur in the wind field over the city. These circulations result in concentrating aerosol inside them. This effect can explain the small value of the pollution balance of this city.[48]
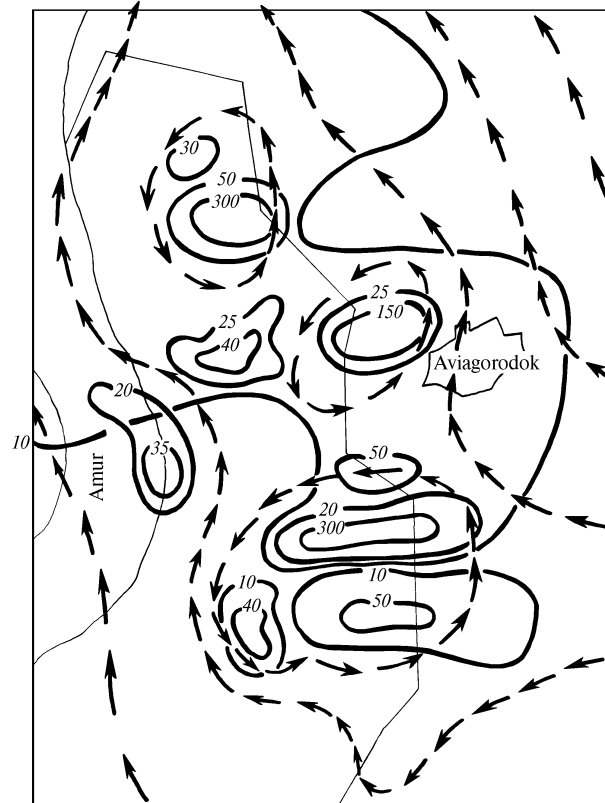

FIG. 12. Distribution of aerosol particle number density (bold solid line) and flow lines (arrows →) over Khabarovsk; solid line marks the city boundaries.

The third kind of sounding for ecological survey of cities is the determination of the parameters of emission from large sources and their composition and amount. Composition and amount of emission are usually calculated on the basis of the technology or determined by collecting samples from the smoke stacks. In this case the physicochemical changes which may occur in the composition of gas—aerosol mixture spreading through the stack and entering the atmosphere are not taken into account.

It should be noted that a lot of measurements were performed with the aircraft—laboratory flying in the emission plumes. But, as a rule, they were of particular character and reduced either to the detection of one or several emission components or to the investigation of their dynamics in the plume.[43—46,52,53] Such measurements gave no way of deducing a general concept of a large number of substances and amount of their emission. The equipment of the "OPTIK—E" AN—30 aircraft—laboratory[1,11] is capable of obtaining a large bulk of information about the emission characteristics.

The sounding of emission of large industrial enterprises was carried out by the scheme shown in Fig. 11c or by the

direct collection of air samples when flying through the plume or with a lidar when flying over the plume.[54] The samples were collected near the stacks at distances of 100–200 m from their edges. The altitude and direction of the flight were hold in such a manner that the aircraft–laboratory flew through the plume center perpendicularly to it. Filters and containers were exposed only within the plume, the other characteristics were recorded continuously. The results were published in Refs. 42 and 55.

The meteorological and navigation parameters which were simultaneously recorded from onboard the "OPTIK–E" AN–30 aircraft–laboratory[11] made it possible not only to determine the emission composition, but also to calculate its amount for each object.

Knowing the plume parameters, the wind velocity $V(s)$ at the flight altitude, and the mean concentration of pollutants $C_i(s)$ in the plume cross section, we can determine the amount of substance emitted per unit time

$$Q = \int_s \int C_i(s)\, V(s)\, \mathrm{d}\, s.$$

The estimated total error in determining the amount of emission by this method does not exceed 35%.

Without presenting the data on the amount of emission of different objects, we note that the results obtained by the given procedure may differ from the results of calculations based on the technology by a factor from 0.95 to 10. The reasons for these disagreements were discussed at length in Ref. 48, therefore, we will not describe them here.

The ecological survey of cities described in this paper allowed us to obtain a great bulk of actual material which cannot be described in a single paper. Only a small portion of it has been published. To efficiently use the obtained ecological information the database was created[56] which was included in the list of Information Center of the National Committee of the Russian Academy of Sciences under the International Geosphere–Biosphere Program.

CONCLUSION

This review includes the results which were obtained under the program of airborne studies of the Institute of Atmospheric Optics only in one field: examination of atmospheric aerosol properties. The data on gas composition of air and industrial emissions as well as those on lidar sounding and spectrophotometry of atmospheric parameters and characteristics of the underlying surface were not considered in this paper. So they should be considered separately.

ACKNOWLEDGMENTS

REFERENCES

1. A.Kh. Khrgian, *Outlines on Development of Meteorology* (Gidrometeoizdat, Leningrad, 1948), 349 pp.
2. A.S. Zaitsev and A.A. Ledokhovich, *Instrumentations and Procedure for Airborne Investigation of Clouds* (Gidrometeoizdat, Leningrad, 1960), 175 pp.
3. B.D. Belan, Atmos. Oceanic Opt. **6**, No. 1, 1–18 (1993).
4. B.D. Belan, in: *Instrumentation for Remote Sounding of Atmospheric Parameters* (Tomsk Affiliate of the Siberian Branch of the Academy of Sciences of the USSR, Tomsk, 1987), pp. 34–40.
5. V.K. Kovalevskii and G.N. Tolmachev, *ibid.*, pp. 40–46.
6. M.V. Panchenko, A.G. Tumakov, and S.A. Terpugova, *ibid.*, pp. 40–46.
7. A.I. Grishin and G.G. Matvienko, *ibid.*, pp. 47–53.
8. A.N. Volkov, D.M. Kabanov, S.M. Sakerin, et al., *ibid.*, pp. 71–81.
9. A.S. Bespalov, E.I. Gromakov, E.V. Pokrovskii, et al., *ibid.*, pp. 59–71.
10. A.M. Abramochkin, V.V. Zanin, I.E. Penner, et al., Opt. Atm. **1**, No. 2, 92–96 (1988).
11. V.E. Zuev, B.D. Belan, D.M. Kabanov, et al., Atmos. Oceanic Opt. **5**, No. 10, 706–711 (1992).
12. N.K. Vinnichenko, N.Z. Pinus, S.M. Shmeter, and G.N. Shur, *Turbulence in a Free Atmosphere* (Gidrometeoizdat, Leningrad, 1976), 187 pp.
13. V.V. Pavlov, Meteorol. Gidrol., No. 3, 63–68 (1985).
14. T.E. Graedal and J.P. Franey, J. Geophys. Res. **79**, No. 36, 5643–5645 (1974).
15. A.S. Monin, *Weather Forecast as a Problem of Physics* (Nauka, Moscow, 1969), 184 pp.
16. B.D. Belan, A.I. Grishin, G.O. Zadde, and G.G. Matvienko, Izv. Akad. Nauk SSSR, Fiz. Atmos. Okeana **23**, No. 4, 402–408 (1987).
17. B.D. Belan, Atmos. Oceanic Opt. **7**, No. 8, 558–562 (1994).
18. B.D. Belan, A.I. Grishin, G.G. Matvienko, and I.V. Samokhvalov, *Spatial Variability of Atmospheric Aerosol Characteristics* (Nauka, Novosibirsk, 1989), 152 pp.
19. B.D. Belan, O.Yu. Luk'yanov, M.K. Mikushev, et al., Atmos. Oceanic Opt. **5**, No. 10, 701–705 (1992).
20. G.M. Krekov and R.F. Rakhimov, *Optical Models of Atmospheric Aerosol* (Tomsk Affiliate of the Siberian Branch of the Academy of Sciences of the USSR, Tomsk, 1986), 159 pp.
21. B.D. Belan, G.O. Zadde, Yu.A. Pkhalagov, and T.M. Rasskazchikova, Izv. Akad. Nauk SSSR, Fiz. Atmos. Okeana **23**, No. 6, 622–628 (1987).
22. B.D. Belan, E.V. Pokrovskii, and V.V. Tokarev, in: *Proceedings of the 12th Meeting on Actinometry*, Irkutsk (1984), pp. 200–203.
23. B.D. Belan, G.O. Zadde, M.V. Panchenko, et al., in: *Abstracts of Reports at the All–Union Conference "Transformation and Far Transfer of Gaseous and Aerosol Admixtures in the Atmosphere"*, Vil'nyus (1986), pp. 112–113.
24. B.D. Belan, G.O. Zadde, M.V. Panchenko, et al., in: *Proceedings of XI All–Union Symposium on Laser and Acoustic Sounding of the Atmosphere* (1987), Vol. 1, pp. 125–129.
25. B.D. Belan, D.M. Kabanov, M.V. Panchenko, et al., in: *Soviet–American Experiment on Studying Arid Aerosol* (Gidrometeoizdat, Leningrad, 1992), pp. 26–38.
26. A.V. Andronova, B.D. Belan, D.A. Gillette, et al., Izv. Akad. Nauk SSSR, Fiz. Atmos. Okeana **28**, No. 8, 798–804 (1992).
27. M.A. Sviridenkov, D.A. Gillette, A.A. Isakov, et al., Atmos. Environ. **270A**, No. 16, 2481–2487 (1993).
28. B.D. Belan, G.O. Zadde, M.V. Panchenko, et al., Atm. Opt. **2**, No. 8, 661–665 (1989).
29. I.P. Mazin, Meteorol. Gidrol., No. 1, 54–61 (1982).
30. B.D. Belan, G.O. Zadde, and T.M. Rasskazchikova, Meteorol. Gidrol., No. 4, 38–46 (1987).
31. B.D. Belan, M.V. Panchenko, T.M. Rasskazchikova, and V.V. Pol'kin, in: *Proceeding of the 9th All–Union Symposium on Laser and Acoustic Sounding of the Atmosphere*, Tomsk (1987), Vol. 1, pp. 130–133.

32. V.E. Zuev, V.V. Antonovich, B.D. Belan, et al., Dokl. Ross. Akad. Nauk **325**, No. 6, 1146—1150 (1992).

33. B.D. Belan and G.O. Zadde, Dokl. Akad. Nauk SSSR **290**, No. 6, 3128—3131 (1986).

34. B.D. Belan, G.O. Zadde, V.K. Kovalevskii, et al., Atm. Opt. **1**, No. 6, 67—77 (1988).

35. B.D. Belan, G.O. Zadde, M.V. Panchenko, et al., Meteorol. Gidrol., No. 8, 39—48 (1988).

36. V.E. Zuev, B.D. Belan, G.O. Zadde, et al., Izv. Akad. Nauk SSSR, Fiz. Atmos. Okeana **24**, No. 9, 967—972 (1988).

37. V.E. Zuev, B.D. Belan, V.V. Veretennikov, et al., Atm. Opt. **2**, No. 7, 605—609 (1989).

38. V.E. Zuev, B.D. Belan, and G.O. Zadde, *Optical Weather* (Nauka, Novosibirsk, 1990), 192 pp.

39. S.M. Shmeter, *Thermodynamics and Physics of Convective Clouds* (Gidrometeoizdat, Leningrad, 1987), 288 pp.

40. L.S. Dubrovina, *Clouds and Precipitation from Airborne Sounding Data* (Gidrometeoizdat, Leningrad, 1983), 216 pp.

41. I.P. Mazin and S.M. Shmeter, *Clouds, Construction and Physics of Formation* (Gidrometeoizdat, Leningrad, 1983), 280 pp.

42. B.D. Belan, V.V. Burkov, M.V. Panchenko, et al., Atmos. Oceanic Opt. **5**, No. 2, 121—125 (1992).

43. A. Despres and F. Rancillac, Pollut. Atmosph., No. 7—9, 226—236 (1987).

44. V.A. Dyachuk and L.A. Ramenskii, Trudy Ukr. Nauchno—Issled. Gidrometeorol. Ins. No. 241, 3—10 (1991).

45. E.P. Volkov, *Monitoring of Pollutions of Thermal Electric Power Plant Discharges* (Energoatomizdat, Moscow, 1986), 256 pp.

46. M. Tanaka, T. Nakazawa, S. Aoki, and H. Ohshima, Tellus **B40**, No. 1, 16—22 (1988).

47. Yu.A. Izrael', I.M. Nazarov, Sh.D. Fridman, et al., *Monitoring of Transboundary Transport of Air Pollutants* (Gidrometeoizdat, Leningrad, 1987), 303 pp.

48. B.D. Belan, Atmos. Oceanic Opt. **6**, No. 2, 124—135 (1993).

49. A.M. Vladimirov, Yu.I. Lyakhin, L.T. Matveev, and V.G. Orlov, *Environmental Protection* (Gidrometeoizdat, Leningrad, 1991), 424 pp.

50. V.E. Zuev, B.D. Belan, G.O. Zadde, et al., Atm. Opt. **2**, No. 6, 523—526 (1989).

51. B.D. Belan, M.K. Mikushev, M.V. Panchenko, et al., *ibid*. **4**, No. 9, 697—703 (1991).

52. L.I. Boltneva, P.A. Bryukhanov, I.M. Nazarov, et al., Tr. Ins. Prikl. Geofiz., No. 71, 143—149 (1988).

53. B. Abramovskii, in: *Problems of Background Monitoring of Environment*, No. 4, 181—193 (1986).

54. V.E. Zuev, B.V. Kaul', I.V. Samokhvalov, et al., *Laser Sounding of Industrial Aerosols* (Nauka, Novosibirsk, 1986), 108 pp.

55. B.D. Belan, V.I. Vaver, V.K. Kovalevskii, et al., Atmos. Oceanic Opt. **6**, No. 5, 332—352 (1993).

56. B.D. Belan, A.V. Ligotskii, O.Yu. Luk'yanov, et al., Atmos. Oceanic Opt. **7**, No. 8, 585—590 (1994).